

017851  
P.14

NASA Technical Memorandum 102369

# Design of Ceramic Components With the NASA/CARES Computer Program

Noel N. Nemeth  
*Aerospace Design & Fabrication, Inc.*  
*Lewis Research Center*  
*Cleveland, Ohio*

and

Jane M. Manderscheid and John P. Gyekenyesi  
*National Aeronautics and Space Administration*  
*Lewis Research Center*  
*Cleveland, Ohio*

April 1990

(NASA-TM-102369)	DESIGN OF CERAMIC	N90-26359
COMPONENTS WITH THE NASA/CARES COMPUTER		
PROGRAM (NASA) 14 p	CSCS 20K	
		Unclass
		G3/39 0292962



**ORIGINAL CONTAINS  
COLOR ILLUSTRATIONS**

## **Design of Ceramic Components With the NASA/CARES Computer Program**

Noel N. Nemeth  
Aerospace Design & Fabrication, Inc.  
Lewis Research Center  
Cleveland, Ohio 44135

and

Jane M. Manderscheid and John P. Gyekenyesi  
National Aeronautics and Space Administration  
Lewis Research Center  
Cleveland, Ohio 44135

### **Summary**

This report describes the ceramics analysis and reliability evaluation of structures (CARES) computer program. The primary function of the code is to calculate the fast-fracture reliability or failure probability of macroscopically isotropic ceramic components. These components may be subjected to complex thermomechanical loadings, such as those found in heat engine applications. CARES uses results from MSC/NASTRAN or ANSYS finite-element analysis programs to evaluate how inherent surface and/or volume type flaws affect component reliability. CARES utilizes the Batdorf model and the two-parameter Weibull cumulative distribution function to describe the effects of multiaxial stress states on material strength. The principle of independent action (PIA) and the Weibull normal stress averaging models are also included. Weibull material strength parameters, the Batdorf crack density coefficient, and other related statistical quantities are estimated from four-point bend bar or uniform uniaxial tensile specimen fracture strength data. Parameter estimation can be performed for a single or multiple failure modes by using a least-squares analysis or a maximum likelihood method. Kolmogorov-Smirnov and Anderson-Darling goodness-of-fit tests, 90-percent confidence intervals on the Weibull parameters, and Kanofsky-Srinivasan 90-percent

confidence band values are also provided. Examples are provided to illustrate the various features of CARES.

### **Introduction**

The unique properties that advanced ceramics offer in the areas of high-temperature strength, environmental resistance, and low density provide the potential for greatly increased fuel efficiency and reduced emissions in aerospace and automotive engine applications. Consequently, research has focused on improving ceramic material processing and properties as well as on establishing a sound design methodology.

Because of the variable severity of inherent flaws, the nature of ceramic failure is probabilistic and optimization of design requires the ability to accurately determine a loaded component's reliability. Methods of quantifying this reliability and the corresponding failure probability have been investigated and refined by the authors. The result of this effort is a public domain computer program with the acronym CARES<sup>1</sup> (ceramics analysis and reliability evaluation of structures). CARES (ref. 1) calculates the fast fracture reliability of macroscopically isotropic ceramic components. These

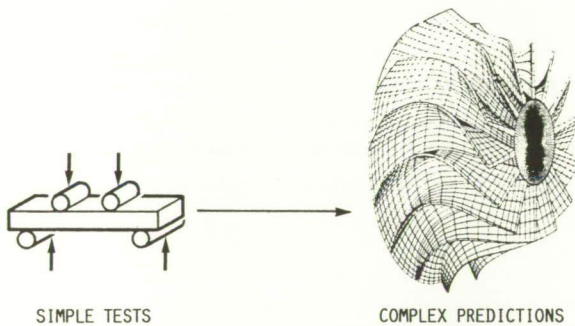
<sup>1</sup>Formerly SCARE (structural ceramics analysis and reliability evaluation).

components may be subjected to complex thermomechanical loadings such as those found in heat engine applications.

The design methodology used by CARES combines three major elements: (1) linear elastic fracture mechanics (LEFM) theory which relates the strength of ceramics to the size, shape, and orientation of critical flaws, (2) extreme value statistics to obtain the characteristic flaw size distribution function, which is a material property, and (3) material microstructure. Inherent in this design procedure is that component integrity is a function of the entire field solution of the stresses and is not based only on the most highly stressed point. In addition, the size of the stressed material surface area and volume affect the component strength.

Probabilistic component design requires the determination of the fracture strength distribution from simple geometry flexural or tensile test specimens. The statistical material parameters are estimated as functions of temperature, specimen loading, and geometry. From these data the reliability for a complex component geometry and loading is then predicted (fig. 1). Appropriate design changes are made until an acceptable probability of failure has been reached.

- CERAMICS ARE BRITTLE AND HAVE MANY FLAWS
- RANDOM FLAW SIZE AND ORIENTATION REQUIRE PROBABILISTIC METHOD
- APPROACH:



- REQUIRES ENTIRE STRESS FIELD, NOT MAXIMUM STRESS POINT

Figure 1.—CARES uses statistical material strength parameters determined from simple tests to predict the reliability of complex ceramic components.

## Program Capability and Description

CARES is an integrated computer program written in FORTRAN 77 which uses Weibull (refs. 2 and 3) and Batdorf (refs. 4 and 5) fracture statistics to predict the fast fracture reliability of isotropic ceramic components. CARES has three primary functions: (1) to analyze statistically the data obtained from the fracture of simple uniaxial tensile or flexural specimens, (2) to estimate the Weibull and Batdorf material parameters using these data, and (3) to perform a fast fracture reliability evaluation of a ceramic component experiencing thermomechanical loading. Component reliability is predicted using elastostatic finite-element analysis output from the MSC/NASTRAN or ANSYS computer programs.

The CARES code includes a number of fracture theories to predict material response due to multiaxial stresses. These methods are summarized in table I. The Batdorf (ref. 5) method is recommended because it couples LEFM with the Weibull weakest link theory (WLT) (ref. 2). The Weibull normal stress averaging method (ref. 3) and the principle of independent action (PIA) (refs. 6 and 7) theories are included for comparison purposes and because of their previous popularity. All the fracture models available in CARES use the Weibull two-parameter probability of strength distribution.

Figure 2 shows the fracture criteria and crack geometries available to the user for both surface and volume distributed flaws. The PIA and Weibull normal stress averaging fracture theories do not require a crack geometry. Batdorf's fracture theory can be used with several different mixed-mode fracture criteria and crack geometries. For coplanar crack extension, CARES uses the total strain energy release rate theory. Out-of-plane crack extension criteria are approximated by a simple semiempirical equation (refs. 8 and 9). This equation involves a parameter which can be used to approximate various mixed-mode theories or experimental results. For comparison, Griffith's maximum tensile stress analysis for volume flaws is also included. The highlighted boxes in figure 2 show the recommended fracture criteria and flaw shapes.

The statistical material parameters are obtained from the fracture stresses of many test specimens (ideally 30 or more) of fixed geometry and loading. Solutions for the four-point

TABLE I.—STATISTICAL FAST FRACTURE MODELS AVAILABLE WITH CARES

Weakest link fracture model	Size effect	Stress state effects	Computational simplicity	Theoretical basis
Weibull (1939)	Yes ↓	Uniaxial	Simple	Phenomenological
Normal stress averaging (1939)		Multiaxial	Complex	
Principle of independent action (1967)		Multiaxial	Simple	Maximum principal stress theory
Batdorf:				
Shear-insensitive (1974)		Multiaxial	Complex	Linear elastic fracture mechanics
Shear-sensitive (1978)				

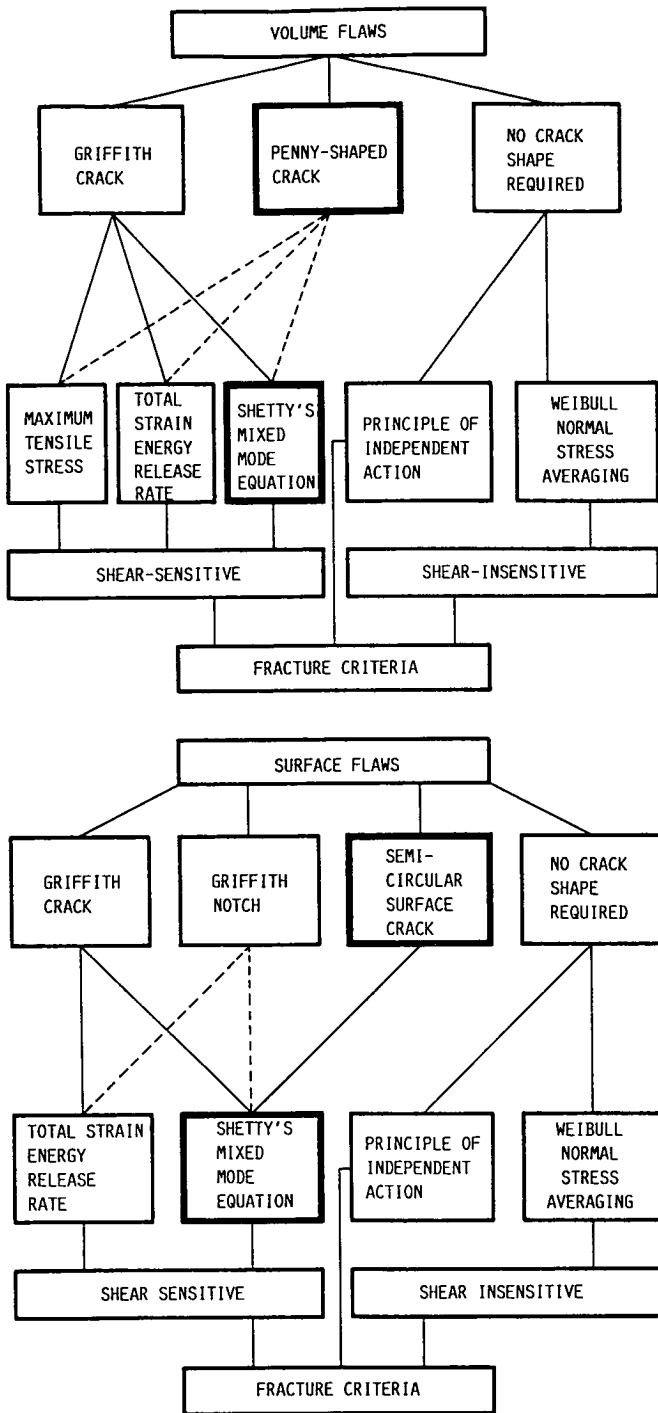


Figure 2.—Available failure criteria and crack shapes. (Recommended failure criteria and crack shapes are highlighted.)

modulus of rupture (MOR) bending bar (ref. 10) and the pure tensile specimen (ref. 11) tested at a user specified temperature have been incorporated in the CARES program. Since the statistical material parameters are a function of temperature, up to 20 data sets may be input at discrete temperature levels. Lagrangian polynomials are utilized to interpolate the

parameter values at other temperatures. Each data set may consist of up to 200 specimen fracture stresses. Each specimen can be identified by its mode of failure—either volume flow, surface flaw, or unknown—so that statistical parameters from competing failure modes can be estimated.

CARES can identify potential bad fracture stress data (outliers). The outlier test developed by Stefansky (ref. 12) and subsequently used by Neal et al. (ref. 13) is employed. The test can detect multiple outliers from a sample of up to 100 specimens at either the 1-, 5-, or 10-percent significance levels. Data detected as outliers are flagged with a warning message and any further action is left to the discretion of the user.

Weibull parameters are obtained as a function of the specimen surface and/or volume as requested by the user. Biased estimates of the Weibull parameters are obtained from either least-squares analysis or the maximum likelihood method for complete or censored samples (competing failure modes). CARES uses the Weibull log likelihood equations given in Nelson (ref. 14) and the rank increment adjustment method described by Johnson (ref. 15).

Because the estimates of statistical parameters are obtained from a finite amount of data, they contain an inherent uncertainty which can be characterized by bounds in which the true parameters are likely to lie. For the maximum likelihood method the 5- and 95-percentile confidence limits for the Weibull parameters are provided (ref. 16).

The ability of the probability distribution calculated from the Weibull parameters to reasonably fit the experimental data is measured with the Kolmogorov-Smirnov (K-S) and Anderson-Darling (A-D) goodness-of-fit tests. These tests are discussed by D'Agostino and Stephens (ref. 17). The A-D test is provided because it is more sensitive to discrepancies at low and high probabilities of failure than the more commonly used K-S test. The Kanofsky-Srinivasan 90-percent confidence band values (ref. 18) about the Weibull line are given as an additional test of the fit of the data to the Weibull distribution.

Figure 3 illustrates the operational flow of the program. For a finite-element model, reliability calculations are performed at the element level and the overall component reliability is then the product of all the element survival probabilities. Reliability due to the presence of volume flaws is calculated from the volume statistical material strength parameters and the output of the stresses, volumes, and temperatures from isoparametric brick, wedge, or axisymmetric finite elements. Reliability evaluation due to the presence of surface flaws is calculated from the surface statistical material strength parameters and the output of the two-dimensional surface stresses, areas, and temperatures from isoparametric quadrilateral and triangular shell elements. Solid elements are used for the structural modeling. Shell elements are only used to identify external surfaces of solid elements consistent with the component external boundaries that are required for the reliability analysis.

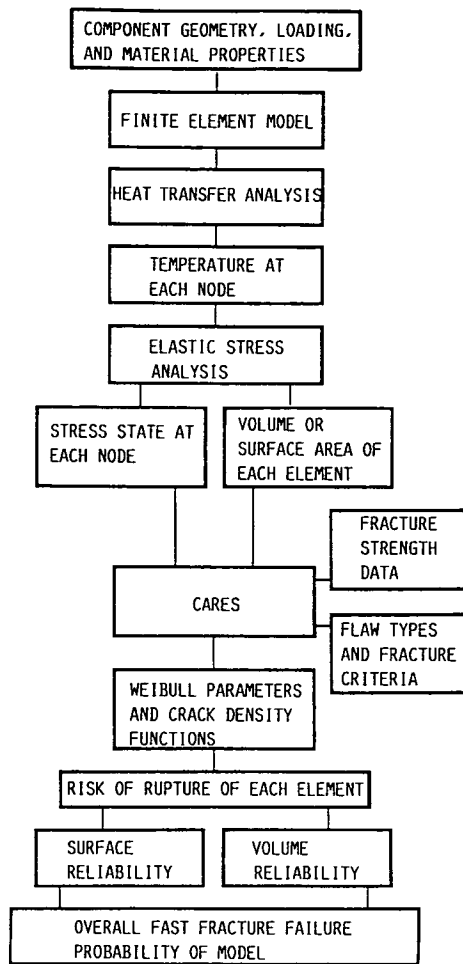


Figure 3.—Block diagram for analysis and reliability evaluation of ceramic components.

Provision is made in CARES to permit the use of cyclic symmetry modeling. CARES also has a multiple material capability; a model can consist of up to 100 different materials (up to 100 different statistical material characterizations). Elements not designated as brittle materials are ignored in the reliability computations. Temperature-dependent statistical material properties are interpolated at each individual element temperature. The risk of rupture intensity is also calculated for each element and these values are sorted to determine the maximum values.

Two versions of the code, designated as CARES1 and CARES2, are available. The CARES1 version assumes that stress and temperature gradients within each element are negligible, and, therefore, only element centroidal principal stresses are used in the reliability calculations. The CARES2 version takes into account element stress gradients by dividing each brick element into 27 subelements and each quadrilateral shell element into 9 subelements. Subelement centroidal principal stresses are then computed and used in the subsequent reliability calculations. CARES2 enables the finite-element

model to consist of fewer elements for the same level of convergence to the true solution as CARES1.

## Input Requirements

To control the execution of the CARES program, an input file must be prepared. On the tape or disks provided with the program is a file called TEMPLET INP that can be used to construct an input file for a particular problem. Input to CARES is keyword driven. Data are input by the user under each keyword. An explanation of the input required or a list of input choices is provided next to the keyword.

The CARES program requires three categories of input: (1) Master Control Input, (2) Material Control Input, which includes temperature-dependent material data, and, optionally, (3) MSC/NASTRAN or ANSYS output data files from finite-element analysis. The Master Control Input is a set of control indices that directs the overall program execution. The Material Control Input consists of control indices and either the data required to estimate the statistical material parameters or direct input of the statistical parameter values themselves for various temperatures. This input category includes the choices of fracture criteria and flaw shapes shown in figure 2. The Master Control Input and the Material Control Input are contained in the TEMPLET INP file. The third input category, MSC/NASTRAN or ANSYS output data files, includes finite-element analysis data files containing the element stresses, volumes/areas, and temperatures.

## Output Information

The first part of the CARES output is an echo of the choices selected (or default values) from the Master Control Input. If a finite-element model reliability analysis is not performed, then CARES proceeds to echo the Material Control Input. If postprocessing of a finite-element model is done, then, for each element, the centroidal or subelement principal stresses with appropriate element area or volume and temperature are listed. The printing of element stress tables in CARES is optional. In addition, two element cross-reference tables are printed. The first table lists the shell element number and gives the corresponding solid element to which it is attached. The second table lists the solid element identification number and lists up to six associated shell elements (a brick element could have all of its six faces as external surfaces).

CARES echoes the user inputs for each section of the Material Control Input. If statistical material parameters are directly input, then output pertaining to calculated values of the normalized Batdorf crack density coefficient  $\bar{k}_B$  will follow. If statistical material parameters are determined from experimental fracture data, then the output will identify the method of solution, the number of specimens in each batch,

and the temperature of each test. In addition, the output echoes the sorted input values of all specimen fracture stresses with proper failure mode identification.

Results from the statistical analysis of the fracture data are then printed. The fracture strength and corresponding significance level are listed for detected outliers followed by the estimated statistical material parameters from least-squares or maximum likelihood analyses. The biased and the unbiased values of the Weibull shape parameter, the specimen Weibull characteristic strength, the upper and lower bound values at 90-percent confidence level for both parameters, the specimen Weibull mean value, and corresponding standard deviation are printed for each specified temperature. For censored statistics these values are generated first for volume flaw analysis and subsequently for the surface flaw analysis. It should be noted that not all the previously mentioned information is available for all methods of material parameter estimation.

The K-S goodness-of-fit test is done for each specimen fracture stress and the corresponding K-S statistics  $D+$ ,  $D-$ , and significance level are listed. Similarly, the K-S statistic for the overall sample set is printed along with the significance level. This overall statistic is the absolute maximum of individual data  $D+$  and  $D-$  factors. For the A-D goodness-of-fit test, the A-D statistic  $A^2$  is determined for the overall population and its associated significance level is printed.

The next table of the output contains data to construct K-S 90-percent confidence bands about the Weibull distribution. The table includes fracture stress data, the corresponding Weibull probability of failure values, the 90-percent upper and lower confidence band values about the Weibull line, and the median rank value for each data point.

The last table from the statistical analysis section of CARES summarizes the material parameters used in component reliability calculations. These parameters, which are listed as a function of temperature, include the biased Weibull modulus, the normalized Batdorf crack density coefficient, and the Weibull scale parameter or the unit volume or unit area characteristic strength, whichever is appropriate. The values printed correspond to the experimental temperatures input and five additional interpolated sets of values between each input temperature. The interpolated parameters are output for checking purposes. Information on the selected fracture criterion and the crack shape is printed as required.

If a component reliability analysis with finite-element data is being performed, then tables will be generated to summarize the reliability evaluation of each finite element. One table is provided for volume flaw analysis (solid elements) and one table is given for surface flaw analysis (shell elements) as requested by the user. The tables list the element identification (ID) numbers and the corresponding element material ID, survival probability, failure probability, risk-of-rupture intensity (risk-of-rupture divided by element volume or area), and temperature-interpolated statistical material parameters. Following each table is a sorted list of the 15 most critical

risk-of-rupture intensity values and corresponding element numbers. Also included is the probability of failure and survival for the component surface or volume, whichever is appropriate. Finally, the overall component probability of failure and the component probability of survival are printed.

## Theory

The first probabilistic approach used to account for the scatter in fracture strength of brittle materials was introduced by Weibull (refs. 2 and 3). This approach is based on the previously developed weakest link theory (WLT) (refs. 19 to 21), which is primarily attributed to Pierce who proposed it while modeling yarn failure. The WLT is analogous to pulling a chain where catastrophic failure occurs when the weakest link in the chain breaks. The reliability of the chain is the product of the survival probabilities of the individual links.

Phenomenological observations indicate that monolithic ceramic failures behave in accordance with WLT. For a ceramic component containing volume flaws and loaded in uniaxial tension, the probability of survival is expressed as

$$P_{sV} = \exp \left\{ - \left[ \int_V N_V(\sigma) dV \right] \right\} \quad (1)$$

where  $V$  is the component volume and the subscript  $V$  denotes volume-dependent terms. The function  $N_V(\sigma)$ , referred to as the crack density function, represents the number of flaws per unit volume having a strength equal to or less than  $\sigma$ . The value of the integral is called the risk-of-rupture.

Weibull introduced a three-parameter power function for the crack density function  $N_V(\sigma)$ :

$$N_V(\sigma) = \left( \frac{\sigma - \sigma_{uV}}{\sigma_{oV}} \right)^{m_V} \quad (2)$$

where  $\sigma_{uV}$  is the threshold stress (location parameter), usually taken as zero for ceramics. The location parameter is the value of applied stress below which the failure probability is zero. When the location parameter is zero, the two-parameter Weibull model is obtained. The scale parameter  $\sigma_{oV}$  then corresponds to the stress level where 63.2 percent of specimens with unit volume would fracture. The scale parameter has dimensions of stress  $\times$  (volume)<sup>1/ $m_V$</sup> . The reciprocal of  $\sigma_{oV}^{m_V}$  is called the uniaxial Weibull crack density coefficient  $k_{wV}$ , and  $m_V$  is the shape parameter (Weibull modulus or Weibull slope), which is a measure of the degree of strength dispersion. These statistical parameters are material properties that are temperature and processing dependent. They are evaluated from uniaxial flexure or tensile specimen fracture data.

For surface flaw induced failure in ceramic structures these expressions become a function of the component surface area

A. Herein the subscript  $S$  denotes analogous parameters that are a function of surface area.

To predict material response under multiaxial stress states, Weibull (ref. 3) proposed the normal stress averaging method. While this approach is intuitively plausible, it is somewhat arbitrary. Subsequently, Barnett and Freudenthal (refs. 6 and 7) proposed the PIA model. The PIA fracture theory is the weakest link statistical equivalent of the maximum stress failure theory and is only applicable for tensile states of stress. The Weibull method of averaging the tensile normal stress and the PIA model have been the most widely used methods for brittle material design. However, they do not specify the nature of the defect causing the failure.

Recognizing that brittle fracture is governed by LEFM, Batdorf (refs. 4 and 5) proposed that reliability predictions should be based on a combination of the weakest link theory and fracture mechanics. Conventional fracture mechanics dictates that both the size of the critical crack and its orientation relative to the applied loads determine the fracture stress. However, in brittle ceramics the small critical flaw size and the large number of flaws prevent determining the critical flaw, let alone determining its size and orientation. Instead, the combined probability of the critical flaw being within a certain size range and being oriented so that it may cause fracture is calculated. As flaw sizes correspond to strength levels and since strength is easier to measure than size for these microscopic flaws, the probability of a crack existing within a critical strength range is determined.

The Batdorf theory assumes random flaw orientation and a consistent crack geometry. The component failure probability for volume flaws is expressed as

$$P_{fV} = 1 - \exp \left[ - \int_V \int_0^{\sigma_{e\max}} \frac{\Omega(\Sigma, \sigma_{cr})}{4\pi} \frac{dN_V(\sigma_{cr})}{d\sigma_{cr}} d\sigma_{cr} dV \right] \quad (3)$$

where  $\sigma_{cr}$ , the critical stress, is defined as the remote, uniaxial, fracture strength of a given crack in mode I loading. The solid angle  $\Omega(\Sigma, \sigma_{cr})$  is the area of a unit radius sphere containing all the crack orientations for which  $\sigma_e \geq \sigma_{cr}$  due to the existing stress state  $\Sigma$ . The effective stress  $\sigma_e$  is defined as the equivalent mode I stress on the flaw. The constant  $4\pi$  is the surface area of a unit radius sphere and corresponds to a solid angle containing all possible flaw orientations. The limit of integration  $\sigma_{e\max}$  is the maximum effective stress. The Batdorf crack density function  $N_V(\sigma_{cr})$  is approximated by the power function

$$N_V(\sigma_{cr}) = k_{BV} \sigma_{cr}^{m_V} \quad (4)$$

where the material Batdorf crack density coefficient  $k_{BV}$  and Weibull modulus  $m_V$  are evaluated from experimental uniaxial fracture data. In contrast to the Weibull coefficient  $k_{wV}$ ,

which depends only on the specimen fracture data, the Batdorf coefficient requires a fracture criterion and crack shape.

If a shear-insensitive condition is assumed, fracture occurs when  $\sigma_n = \sigma_e \geq \sigma_{cr}$ , where  $\sigma_n$  is the normal tensile stress on the flaw plane. However, for a flat crack it is known from fracture mechanics analysis that a shear stress  $\tau$  applied parallel to the crack plane (mode II or III) also contributes to fracture. Therefore, for polyaxial stress states, expressing the effective stress  $\sigma_e$  as a function of both  $\sigma_n$  and  $\tau$  is more accurate than assuming shear insensitivity.

The equations derived by Batdorf and Heinisch (ref. 5) are based on self-similar (coplanar) crack extension. However, a flaw experiencing a multiaxial stress state usually undergoes crack propagation initiated at some angle to the flaw plane (noncoplanar crack growth). Shetty (ref. 9) performed experiments on polycrystalline ceramics and glass considering crack propagation as a function of an applied far-field multiaxial stress state. He modified an equation proposed by Palaniswamy and Knauss (ref. 8) to empirically fit experimental data. Using this criterion and a penny-shaped crack we obtain

$$\sigma_e = \frac{1}{2} \left[ \sigma_n + \sqrt{\sigma_n^2 + \left( \frac{4\tau}{\bar{C}(2-\nu)} \right)^2} \right] \quad (5)$$

where  $\nu$  is Poisson's ratio and  $\bar{C}$  is a shear sensitivity constant adjusted to best fit the data. Shetty (ref. 9) found a range of values ( $0.80 \leq \bar{C} \leq 2.0$ ) for the materials he tested which contained large induced flaws. Note also that the CARES code has other fracture criteria and flaw shapes available, as indicated in figure 2.

For mixed-mode fracture due to surface flaws the Batdorf failure probability equation is

$$P_{fS} = 1 - \exp \left[ - \int_A \int_0^{\sigma_{e\max}} \frac{\omega(\Sigma, \sigma_{cr})}{2\pi} \frac{dN_S(\sigma_{cr})}{d\sigma_{cr}} d\sigma_{cr} dA \right] \quad (6)$$

where  $\omega(\Sigma, \sigma_{cr})$  is the total arc length on a unit radius circle on which the projection of the equivalent stress satisfies  $\sigma_e \geq \sigma_{cr}$ , and  $2\pi$  is the perimeter of the circle. The cracks are assumed to be randomly oriented in the plane of the external boundary with their planes normal to the surface.

For noncoplanar crack growth and a semicircular surface crack we obtain for the effective stress

$$\sigma_e = \frac{1}{2} \left[ \sigma_n + \sqrt{\sigma_n^2 + 3.301 \left( \frac{\tau}{\bar{C}} \right)^2} \right] \quad (7)$$

where again  $\bar{C}$  is adjusted to best fit the data.

Selected statistical theories and equations for parameter evaluation are explained in detail in reference 22. Typically,

for brittle materials, the Weibull parameters are determined from simple specimen geometry and loading conditions, such as beams under flexure and either cylindrical or flat specimens under uniform uniaxial tension. The flexural test failure probability can be expressed in terms of the extreme fiber fracture stress  $\sigma_f$  or modulus of rupture  $MOR$  using the two-parameter Weibull form

$$P_f = 1 - \exp \left[ - \left( \frac{\sigma_f}{\sigma_\theta} \right)^m \right] \quad (8)$$

where  $m$  is the Weibull modulus and  $\sigma_\theta$  is the volume or area specimen characteristic strength (characteristic modulus of rupture,  $MOR_o$ ). The Weibull scale parameter  $\sigma_o$  for volume and surface cracks is determined from  $\sigma_\theta$ ,  $m$ , and the specimen geometry and loading. The characteristic strength  $\sigma_\theta$  is defined as the uniform stress or extreme fiber stress at which the probability of failure is 0.6321.

## Example 1—Statistical Material Parameter Estimation

To illustrate the methods used to estimate statistical material parameters, results from the fracture of four-point bend bars broken at NASA Lewis Research Center and analyzed by CARES are compared to results independently obtained by Bruckner-Foit and Munz (ref. 23) for the International Energy Agency (IEA) Annex II agreement (ref. 24). Two different materials were analyzed—namely, a hot isostatic pressed (HIPped) silicon carbide (SiC) from Elektroschmelzwerke Kempten (ESK), West Germany, and a HIPped silicon nitride ( $Si_3N_4$ ) from ASEA CERAMA, Sweden.

The flexure bars were distributed by Oak Ridge National Laboratory (ORNL) to the five participating U.S. laboratories, including NASA Lewis. The bars were fractured at these laboratories, and the fracture stress data sets were returned to ORNL as complete data without censoring for different failure modes. The number of specimens of a particular material given to each U.S. participant was 80.

The results of the 80 silicon carbide flexure bars tested at NASA Lewis were analyzed using the CARES code to calculate the least squares and maximum likelihood estimates (MLE's) of the Weibull parameters. The MLE values from CARES for a complete sample are compared in table II to the values obtained from reference 23. The SiC fracture data are plotted in figure 4 along with the proposed Weibull line and the Kanofsky-Srinivasan 90-percent confidence bands. Since no outliers were detected, all the data are within the 90-percent bands, and the goodness-of-fit significance levels are high, it is concluded that the fracture data show good Weibull behavior.

For the ASEA CERAMA HIPped  $Si_3N_4$  bars fractured at NASA Lewis and subsequently analyzed as a complete sample, the statistical material parameters estimated with CARES and reference 23 are shown at the top of table III. The comparison of the MLE's with reference 23 is very good. When analyzed by CARES as a complete sample, the significance levels of 54 and 35 percent from the K-S and A-D goodness-of-fit tests, respectively, were relatively low, indicating a questionable fit to the proposed Weibull distribution. From the outlier test the highest strength fracture stress was detected to be an outlier at the 1-percent significance level. Several of the lower strengths were flagged as outliers at various significance levels (1, 5, or 10 percent). Figure 5 shows a Weibull plot of the data. In this figure it appears that the data are bimodal with an outlier point at the highest strength.

Because of the observed trends, the data were reanalyzed assuming a censored distribution and removing the highest strength value ( $\sigma_f = 817.2$  MPa) as bad data. Although it is possible that both failure modes were surface induced, for the sake of this example it is assumed that the low strength failures were predominantly due to volume flaws and the high strength specimens predominantly fractured due to surface flaws. Since results from fractography of the individual specimens to identify the various failure modes were not available, the fracture origins had to be arbitrarily assigned prior to parameter estimation. Note that identifying individual specimen flaw origins is especially important for small sample sizes where a plot of the data does not yield clear trends. However, for

TABLE II.—WEIBULL PARAMETERS, CONFIDENCE LIMITS, KOLMOGOROV-SMIRNOV, AND ANDERSON-DARLING TEST RESULTS FOR SILICON CARBIDE FOUR-POINT BEND BAR FRACTURE DATA

[All estimates are biased estimates; 80 samples per material; complete sample analysis.]

Method of analysis	Source of data	Shape parameter, $m$	90-Percent confidence limits on $m$		Characteristic strength, $\sigma_\theta$ , MPa	90-Percent confidence limits on $\sigma_\theta$ , MPa		K-S test statistic, $D$	K-S test significance level, $\alpha$ , percent	A-D test significance level, $\alpha$ , percent
			Upper	Lower		Upper	Lower			
Maximum likelihood	CARES	6.48	7.38	5.52	556	573	539	0.070	83	86
Maximum likelihood	Ref. 23	6.59	7.65	5.61	556	574	539	.063	(a)	(a)
Least squares	CARES	6.59	---	---	555	---	---	.071	81	83

<sup>a</sup>Not available.



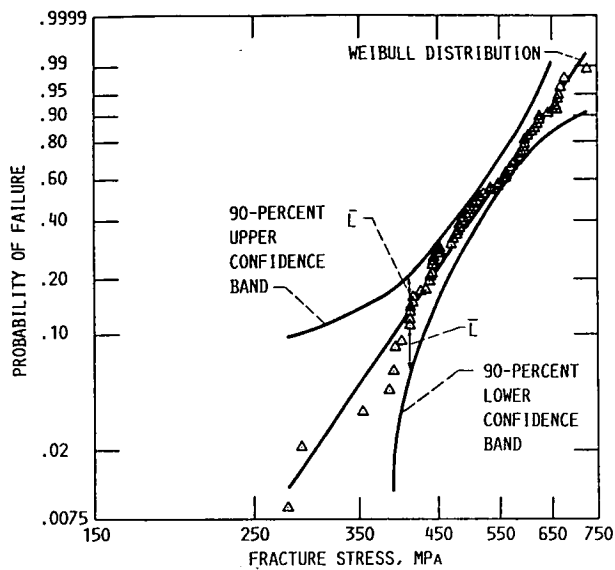


Figure 4.—Weibull distribution and 90-percent confidence bands determined from fracture stress data for ESK HIPped silicon carbide four-point bend bars broken at NASA Lewis (not all data points shown).

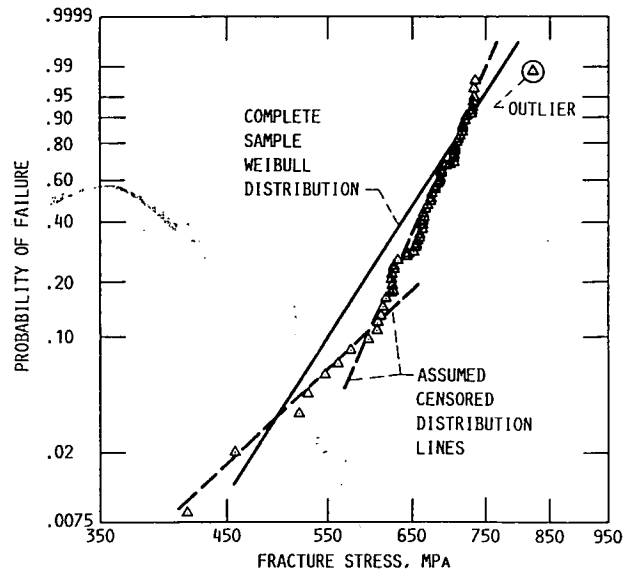


Figure 5.—Complete sample, assumed censored sample Weibull distributions, and outlier determined from fracture stress data for ASEA CERAMA HIPped silicon nitride four-point bend bars broken at NASA Lewis (not all data points shown).

TABLE III.—WEIBULL PARAMETERS, KOLMOGOROV-SMIRNOV, AND ANDERSON-DARLING TEST RESULTS FOR SILICON NITRIDE FOUR-POINT BEND BAR FRACTURE DATA

Method of analysis	Source of data	Assumed distribution	Sample size	Shape parameter, $m$	Characteristic strength, $\sigma_\theta$ , MPa	K-S test statistic, $D$	K-S test significance level, $\alpha$ , percent	A-D test significance level, $\alpha$ , percent
Maximum likelihood	CARES	Surface	80	13.39	686	0.0901	54	35
Maximum likelihood	Ref. 23	↓	80	13.40	686	.088	(a)	(a)
Least squares	CARES		80	11.74	691	.128	15	11
Maximum likelihood	↓	↓	79	16.22	683	.078	73	56
Least squares			79	11.98	688	.124	18	10
Maximum likelihood	↓	Volume	9	4.13	1128	.081	69	58
Least squares		Surface	70	22.81	692	.081	69	58
	Volume	9	6.74	830	.112	28	35	
Maximum likelihood	Surface	70	22.93	691	.112	28	35	
	Volume	13	6.79	876	.074	78	88	
Least squares	Surface	66	21.00	693	.074	78	88	
	Volume	13	6.84	864	.085	62	38	
	↓	Surface	66	15.87	697	.085	62	38

<sup>a</sup>Not available.

the NASA Lewis  $\text{Si}_3\text{N}_4$  data the sample size was large and clear trends could be observed, although extra care is required to determine if the trends are surface or volume flaw based.

Two censored distributions were analyzed. The first was based on an inspection of figure 5, where the lowest nine strengths were assumed due to volume flaws and the remainder due to surface flaws. The second assumed thirteen volume flaws, where the particular volume flaw fracture strengths were assigned such that the MLE's more closely fit the experimental data.

Results of this analysis are shown in table III. At the top of the table are the parameter estimates and goodness-of-fit statistics for the 80-specimen complete sample followed by a complete and censored sample analysis of the data with the outlier removed. The table shows the MLE's along with the least-squares estimates.

When the goodness-of-fit scores are used as the basis of judgement, the censored sample estimated using the maximum likelihood analysis and thirteen volume flaws gives the best fit to the data. The high scores of 78 and 88 for the K-S and

A-D tests, respectively, indicate good Weibull behavior. Improvements in the goodness-of-fit scores may be gained through correctly identifying the location of fracture origins.

It should be noted from figure 5 that the assumed volume flaw distribution dominates the failure response at low probabilities of failure. Therefore, in component design, it is essential to properly account for competing failure modes, otherwise nonconservative design predictions can result.

## Example 2—Rotating Annular Disk

Failure predictions using the available fracture models from CARES, for both volume and surface analysis, were compared to failure predictions obtained by Swank and Williams (ref. 25) for a silicon nitride annular disk rotating at various speeds (fig. 6). The Weibull material parameters were independently evaluated from four-point MOR bar tests using a total of 85 specimens. The Weibull modulus  $m$  was 7.65 and the characteristic modulus of rupture  $MOR_o$  was 808 MPa. If fracture was assumed to be due to volume flaws, then  $\sigma_{oV} = 75 \text{ MPa } (m)^{0.3922}$ ; if fracture was assumed to be due to surface flaws, then,  $\sigma_{oS} = 232 \text{ MPa } (m)^{0.2614}$ . Swank and Williams assumed that both the bars and disks broke because of volume flaws.

Seven disks were fracture tested, and the experimental disk Weibull modulus of 4.95 was considerably different than the 7.65 value based on MOR specimen data. A better agreement between disk and MOR Weibull slopes would lead to improved predictions in failure probabilities for the entire data range. Estimating parameters from small sample sets greatly increases potential deviation from the true population parameters. Confidence limits are used to measure the intrinsic uncertainties in parameter estimates from finite sample sizes. If potential experimental errors are excluded, it is possible that the rotating disks and the MOR bars broke due to the same

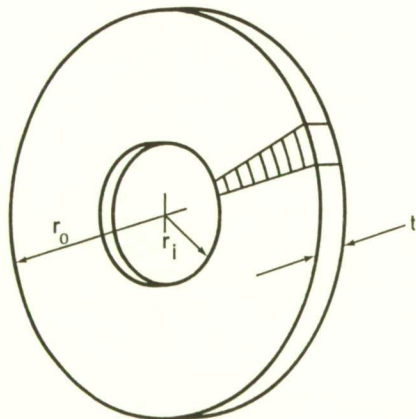


Figure 6.—Rotating annular disk with 15° sector finite-element mesh containing eight brick elements (not to scale). Material, NC-132 hot-pressed  $\text{Si}_3\text{N}_4$ ; inner disk radius,  $r_i$ , 6.35 mm; outer disk radius,  $r_o$ , 41.28 mm; disk thickness,  $t$ , 3.80 mm; RPM range, 70 000 to 114 000.

flaw population because their 90-percent confidence limits overlap between 6.56 and 6.98.

It should be noted that Swank and Williams (ref. 25) also spin tested and performed a volume flaw reliability analysis on a contoured hub and a turbine blade ring geometry. Swank and Williams found that the Weibull moduli obtained from MOR bars cut from the hub and blade ring were in good agreement with the Weibull moduli obtained from the hub and blade ring spin tests, respectively. They also noted that the material parameters used for the annular disk reliability analysis were obtained under less tightly controlled conditions than those used with the other geometries.

All reliability calculations were done with brick and quadrilateral shell elements. Because of symmetry, only 8 solid and 18 shell elements were used in one 15° sector for the model of the disk (fig. 6). Only one element spans both the thickness and circumferential directions. The shell elements were attached to solid elements consistent with the model external surfaces.

Experimental results are plotted in figure 7 along with shear-insensitive (normal stress) and various shear-sensitive predictions from CARES2 for the volume flaw analysis. Results were compared to data calculated by Swank and Williams, who used the Weibull normal stress averaging method and linear axisymmetric finite elements. The agreement between failure predictions is good, with the small discrepancy probably due to the different stress-volume data used in solving the reliability problem.

When using the Batdorf model with CARES there are two methods available to the user to describe the material shear sensitivity. With the input parameter  $IKBAT$  set equal to zero,  $k_B$  is calculated using only the  $\sigma_n$  stress component on the crack plane. This option assumes that mode I fracture is intrinsic to uniaxial loading. When  $IKBAT$  is set equal to one,

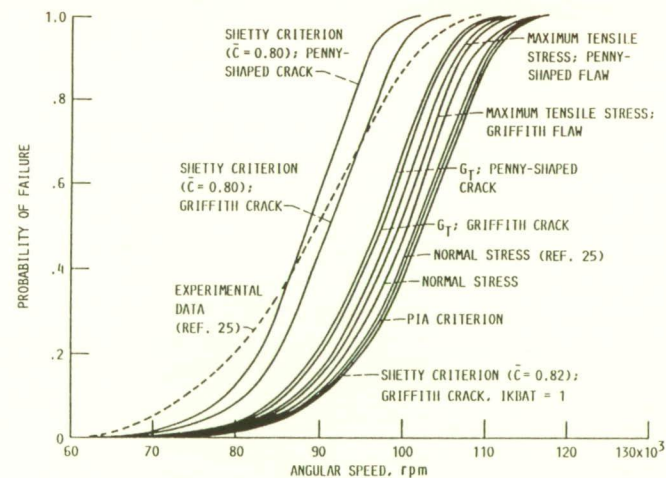


Figure 7.—Comparison of experimental failure probabilities with those for various fracture models for a rotating annular disk (volume flaw analysis):  $m_V = 7.65$ ;  $\sigma_{oV} = 75 \text{ MPa } (m)^{0.3922}$ . For  $IKBAT = 0$ ,  $\bar{k}_{BV} = 16.30$ ; for  $IKBAT = 1$ ,  $\bar{k}_{BV} = 2.99$  (only for Griffith crack, Shetty criterion,  $\bar{C} = 0.82$ );  $G_T$ , total strain energy release rate criterion.

then  $k_B$  is calculated using the user selected fracture criterion and crack geometry. These two methods will yield opposite trends relative to the shear-insensitive criterion as shown in figure 7. When  $IKBAT$  is set equal to zero, the subsequent reliability predictions are more conservative. The value of  $IKBAT$  is chosen so as to best fit the reliability predictions to the experimental data.

For this example the laboratory measurements agree best with the shear-sensitive fracture models using the  $IKBAT = 0$  option. Note that results are given for an approximation of the maximum strain energy release rate criterion  $G_{max}$  using a Griffith crack,  $\bar{C} = 0.82$ , and  $IKBAT = 1$ . Failure probabilities calculated from decreasing shear-sensitive effective stress equations move the probability of failure curves toward the shear-insensitive case. It is observed that Shetty's criterion for  $\bar{C} = 0.80$  and  $IKBAT = 0$  with the penny-shape crack gives the best agreement with experimental data.

The disks were reanalyzed assuming that fractures in the MOR bars as well as the disks were caused by surface flaws. Selected results are shown in figure 8. The same trends are observed for the shear sensitive results as the volume analysis results. However, for a given speed, failure probabilities are significantly less than those obtained by the volume flow analysis for all fracture models, indicating that material failure was most likely due to volume flaws. The main reason for the decreased failure estimates is the much higher equivalent surface Weibull scale parameter  $\sigma_{oS}$ . The importance of post-mortem fractography to identify the nature of the fracture

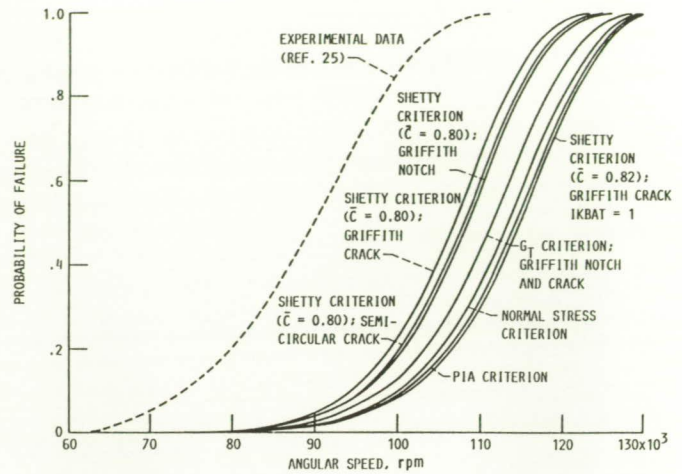


Figure 8.—Comparison of experimental failure probabilities with those for various fracture models for a rotating annular disk (surface flaw analysis):  $m_S = 7.65$ ;  $\sigma_{oS} = 232$  MPa ( $m$ )<sup>0.2614</sup>. For  $IKBAT = 0$ ,  $\bar{k}_{BS} = 4.99$ ; for  $IKBAT = 1$ ,  $\bar{k}_{BS} = 1.76$  (only for Griffith crack, Shetty criterion,  $\bar{C} = 0.82$ );  $G_T$ , total strain energy release rate criterion.

causing flaws is evident from the two different sets of answers in figures 7 and 8.

### Example 3—Si<sub>3</sub>N<sub>4</sub> Mixed Flow Rotor

The CARES code is used by numerous companies worldwide in the automotive, aerospace, nuclear, and computer

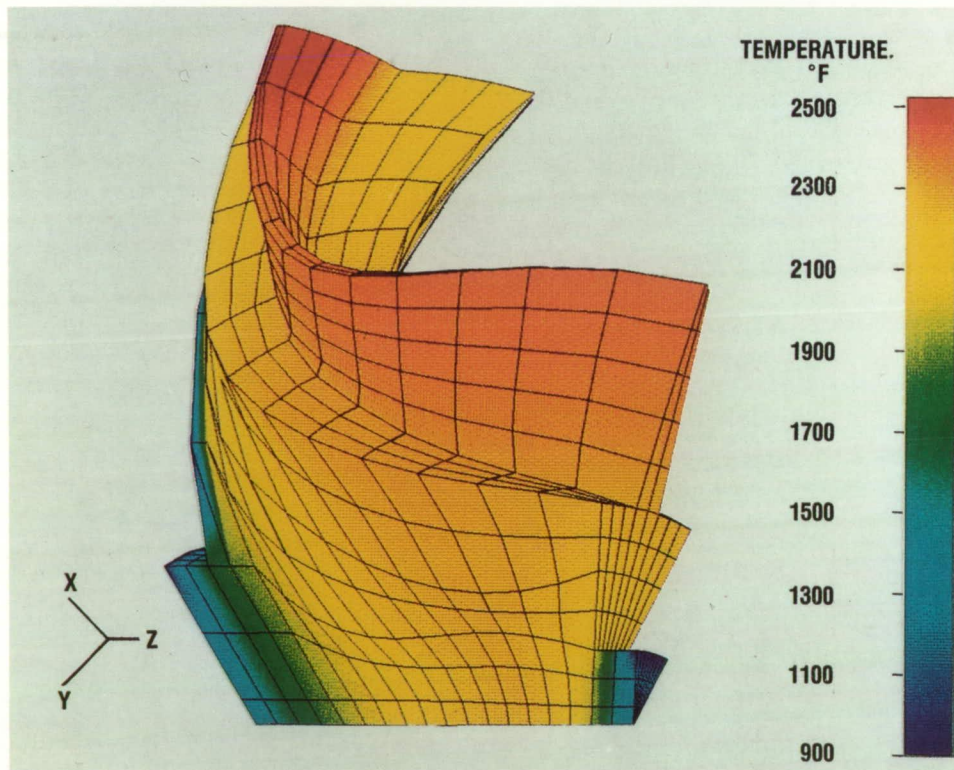


Figure 9.—Silicon nitride mixed-flow rotor temperature distribution.

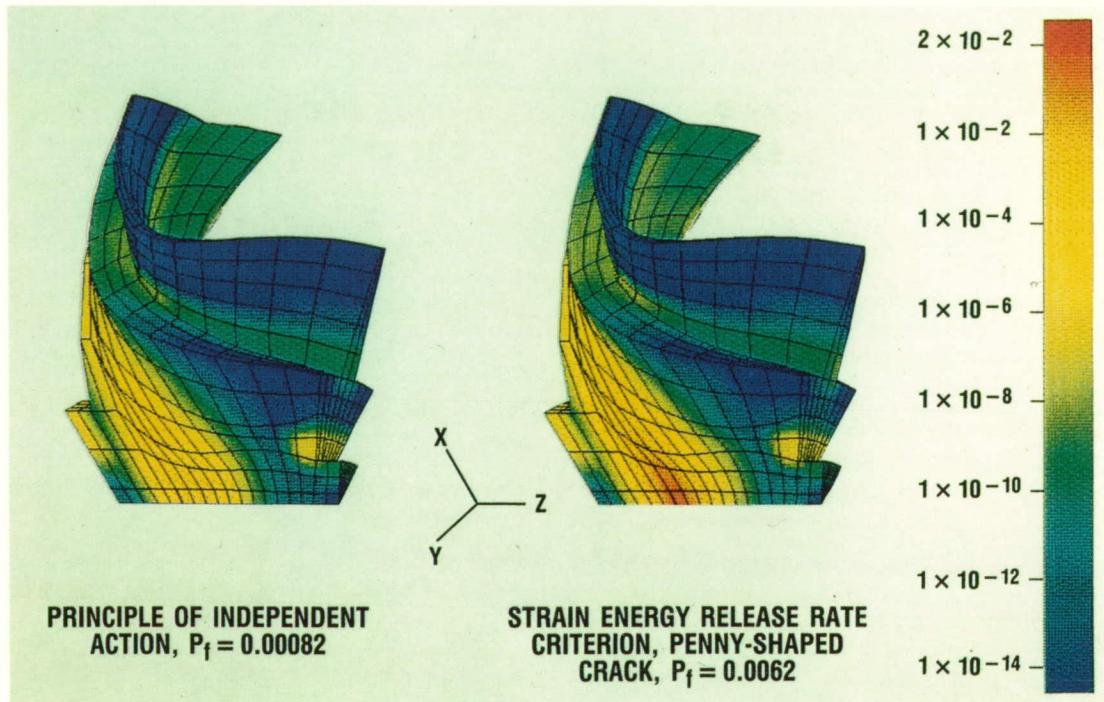


Figure 10.—Volume flow analysis comparison of risk-of-rupture intensities for PIA (left) and total strain energy release rate criterion with a penny-shaped crack geometry and  $IKBAT = 0$  (right).

software fields. At NASA Lewis, CARES has been used for the preliminary design of a silicon nitride mixed-flow rotor for application in small, high-temperature engines. A single blade and a section of the rotor hub were analyzed using the cyclic symmetry option of MSC/NASTRAN.

The results from the heat-transfer analyses are shown in figure 9. In figure 10 the element risk of rupture intensities are plotted from the CARES volume flow analysis for the PIA and the total strain energy release rate criterion using  $IKBAT = 0$  and the penny-shaped crack geometry. Note that the risk of rupture intensity is independent of the individual element geometry, unlike the probability of failure, and provides the designer with a means to visualize the critical stressed regions.

Similar to the rotating annular disk example, the shear-sensitive criterion yields a higher probability of failure for the same applied load. However, the regions of low reliability are the same for both models. This design was optimized to yield a low probability of failure. It is observed in figure 10 that the most critical region is at the rotor hub.

## Conclusions

The potential use of structural ceramics for high-temperature applications depends on the strength, toughness, and reliability of these materials. Components using ceramics can be designed for high reliability in service if the contributing factors that cause material failure are accounted for. This design methodology must combine the statistical nature of strength controlling flaws with fracture mechanics to allow for multiaxial stress states and concurrent flaw populations. This is accomplished using the NASA/CARES public domain computer program for predicting the fast fracture reliability of structural ceramic components. This framework will be subsequently built on to include ceramic fatigue due to subcritical crack growth. The CARES code and accompanying documentation may be obtained by contacting the authors. A PC-based version is also available for statistical analysis and parameter estimation only.

## References

1. Nemeth, N.N.; Manderscheid, J.M.; and Gyekenyesi, J.P.: Ceramic Analysis and Reliability Evaluation of Structures (CARES) User's and Programmer's Manual. NASA TP-2916, 1990.
2. Weibull, W.: A Statistical Theory for the Strength of Materials. Ingeniors Vetenskaps Akadamen Handlingar, No. 151, 1939.
3. Weibull, W.: The Phenomenon of Rupture in Solids. Ingeniors Vetenskaps Akadamen Handlingar, no. 153, 1939.
4. Batdorf, S.B.; and Crose, J.G.: A Statistical Theory for the Fracture of Brittle Structures Subjected to Nonuniform Polyaxial Stresses. *J. Appl. Mech.*, vol. 41, June 1974, pp. 459-464.
5. Batdorf, S.B.; and Heinisch, H.L. Jr.: Weakest Link Theory Reformulated for Arbitrary Fracture Criterion. *J. Am. Ceram. Soc.*, vol. 61, 1978, pp. 355-358.
6. Barnett, R.L., et al.: Fracture of Brittle Materials Under Transient Mechanical and Thermal Loading. U.S. Air Force Flight Dynamics Laboratory, AFFDL-TR-66-220, 1967 (Avail. NTIS, AD-649978).
7. Freudenthal, A.M.: Statistical Approach to Brittle Fracture. *Fracture, An Advanced Treatise*, vol. 2, Mathematical Fundamentals, H. Liebowitz, ed., Academic Press, 1968, pp. 591-619.
8. Palaniswamy, K.; and Kanuss, W.G.: On the Problem of Crack Extension in Brittle Solids Under General Loading. *Mech. Today*, vol. 4, 1978, pp. 87-148.
9. Shetty, D.K.: Mixed-Mode Fracture Criteria for Reliability Analysis and Design with Structural Ceramics. *J. Eng. Gas Turbines Power*, vol. 109, July 1987, pp. 282-289.
10. Baratta, F.I.; Matthews, W.T.; and Quinn, G.D.: Errors Associated with Flexure Testing of Brittle Materials. U.S. Army Materials Technology Laboratory, MTL-TR-87-35, 1987 (Avail. NTIS, AD-A187470).
11. Liu, K.C.; and Brinkman, C.R.: Tensile Cyclic Fatigue of Structural Ceramics. Proceedings of the Twenty-Third Automotive Technology Development Contractors' Coordination Meeting, Society of Automotive Engineers, Warrendale, PA, 1986, pp. 279-284.
12. Stefansky, W.: Rejecting Outliers in Factorial Designs. *Technometrics*, vol. 14, no. 2, 1972, pp. 469-479.
13. Neal, D.; Vangel, M.; and Todt, F.: Statistical Analysis of Mechanical Properties. *Engineered Materials Handbook*, vol. 1, Composites, ASM International, Metals Park, OH, 1987, pp. 302-307.
14. Nelson, W.: *Applied Life Data Analysis*. Wiley, 1982, pp. 333-395.
15. Johnson, L.G.: *The Statistical Treatment of Fatigue Experiments*. Elsevier, 1964, pp. 37-41.
16. Thoman, D.R.; Bain, L.J.; and Antle, C.E.: Inferences on the Parameters of the Weibull Distribution. *Technometrics*, vol. 11, 1969, pp. 445-460.
17. D'Agostino, R.B.; and Stephens, M.A., eds.: *Goodness-of-Fit Techniques*. Marcel Dekker, 1986, pp. 97-193.
18. Kanofsky, P.; and Srinivasan, R.: An Approach to the Construction of Parametric Confidence Bands on Cumulative Distribution Functions. *Biometrika*, vol. 59, no. 3, 1972, pp. 623-631.
19. Pierce, F.T.: Tensile Tests for Cotton Yarns, V. The 'Weakest Link' Theorems on the Strength of Long and of Composite Specimens. *J. Textile Inst.*, vol. 17, 1926, pp. T355-T368.
20. Kontorova, T.A.: A Statistical Theory of Mechanical Strength. *J. Tech. Phys. (USSR)*, vol. 10, 1940, pp. 886-890.
21. Frenkel, J.I.; and Kontorova, T.A.: A Statistical Theory of the Brittle Strength of Real Crystals. *J. Phys. (USSR)*, vol. 7, 1943, pp. 108-114.
22. Pai, S.S.; and Gyekenyesi, J.P.: Calculation of the Weibull Strength Parameters and the Batdorf Flaw-Density Constants for Volume- and Surface-Flaw-Induced Fracture in Ceramics. NASA TM-100890, 1988.
23. Bruckner-Foit, A.; and Munz, D.: Statistical Analysis of Flexure Strength Data, IEA Annex II, Subtask 4. Institute fur Zuverlassigkeit und Schadenskunde in Maschinenbau, University of Karlsruhe, Karlsruhe, West Germany, 1988.
24. Tennery, V.J.: IEA Annex II Management, Subtask 4 Results. Ceramic Technology for Advanced Heat Engines Project. Semiannual Progress Report (Oct. 1986-Mar. 1987). ORNL/TM-10469, Oak Ridge, TN, 1987.
25. Swank, L.R.; and Williams, R.M.: Correlation of Static Strengths and Speeds of Rotational Failure of Structural Ceramics. *Am. Ceram. Soc. Bull.*, vol. 60, no. 8, 1981, pp. 830-834.

1. Report No. NASA TM-102369		2. Government Accession No.		3. Recipient's Catalog No.	
4. Title and Subtitle Design of Ceramic Components With the NASA/CARES Computer Program				5. Report Date April 1990	
				6. Performing Organization Code	
7. Author(s) Noel N. Nemeth, Jane M. Manderscheid, and John P. Gyekenyesi				8. Performing Organization Report No. E-5038	
				10. Work Unit No. 510-01-0A	
9. Performing Organization Name and Address National Aeronautics and Space Administration Lewis Research Center Cleveland, Ohio 44135-3191				11. Contract or Grant No.	
				13. Type of Report and Period Covered Technical Memorandum	
12. Sponsoring Agency Name and Address National Aeronautics and Space Administration Washington, D.C. 20546-0001				14. Sponsoring Agency Code	
15. Supplementary Notes Noel N. Nemeth, Aerospace Design & Fabrication, Inc., Lewis Research Center, Cleveland, Ohio 44135; Jane M. Manderscheid and John P. Gyekenyesi, Lewis Research Center.					
16. Abstract <p><del>This report describes</del> the ceramics analysis and reliability evaluation of structures (CARES) computer program. The primary function of the code is to calculate the fast-fracture reliability or failure probability of macroscopically isotropic ceramic components. These components may be subjected to complex thermomechanical loadings, such as those found in heat engine applications. CARES uses results from MSC/NASTRAN or ANSYS finite-element analysis programs to evaluate how inherent surface and/or volume type flaws affect component reliability. CARES utilizes the Batdorf model and the two-parameter Weibull cumulative distribution function to describe the effects of multiaxial stress states on material strength. The principle of independent action (PIA) and the Weibull normal stress averaging models are also included. Weibull material strength parameters, the Batdorf crack density coefficient, and other related statistical quantities are estimated from four-point bend bar or uniform uniaxial tensile specimen fracture strength data. Parameter estimation can be performed for a single or multiple failure modes by using a least-squares analysis or a maximum likelihood method. Kolmogorov-Smirnov and Anderson-Darling goodness-of-fit tests, 90-percent confidence intervals on the Weibull parameters, and Kanofsky-Srinivasan 90-percent confidence band values are also provided. Examples are provided to illustrate the various features of CARES.</p>					
17. Key Words (Suggested by Author(s)) Ceramic design; Fast fracture; Weibull; Ceramic strength; MOR bars; Censored data; Least squares; Maximum likelihood; Finite elements; Batdorf; MSC/NASTRAN; ANSYS; SCARE; CARES			18. Distribution Statement Unclassified - Unlimited Subject Category 39		
19. Security Classif. (of this report) Unclassified		20. Security Classif. (of this page) Unclassified		21. No. of pages 12	22. Price* A03